 ©2012 Kvantovaya Elektronika and Turpion Ltd

OPTICAL COMMUNICATIONS

PACS numbers: 42.79.Sz; 42.81.Uv; 89.70.Kn
DOI: 10.1070/QE2012v042n07ABEH014862

Direct modelling of error statistics for data transmission through a high data rate communication line using a four-level phase modulation format

A.A. Redyuk, A.S. Skidin, A.V. Shafarenko, M.P. Fedoruk

Abstract. **This paper presents mathematical modelling results for information transmission by optical pulses through a fibre-optic communication line at a rate of 80 Gbit s^{-1} per WDM channel using a four-level phase modulation format. We examine the influence of nonlinear effects on the profile of optical pulses propagating along the fibre. Using direct optical signal detection, we analyse error statistics and demonstrate an uneven error distribution over various symbol combinations.**

Keywords: *fibre-optic communication line, nonlinear distortions, four-level phase modulation format, mathematical modelling.*

1. Introduction

The continuing growth in data traffic through fibre-optic communication lines (FOCLs) has stimulated the search for ways of increasing their transmission capacity. It is known that this can be achieved by increasing both the number of WDM channels combined within one fibre and the channel data rate. To increase the number of channels per fibre, research effort has focused on the development of fibres with new transmission windows where the optical signal attenuation would be under 0.2 dB km^{-1} [1]. Attention has also been paid to assessing the feasibility of reducing the spectral width of neighbouring channels. At the same time, increasing the number of channels leads to an increase in the power that should be coupled into the fibre, which boosts the influence of nonlinear effects on the propagation of optical pulses. To increase the channel data rate, use is made of multilevel phase modulation formats [2]. The feasibility of employing such formats in fibre optics is currently the subject of intense research owing to advances in coherent optical detection [3, 4]. Thus, the considerable increase in the influence of nonlinear effects on data transfer is due to the increase in the signal power coupled into the fibre, the increase in symbol rate from 10 to 100 GBd per WDM channel and the use of nonbinary data transmission formats.

One possible consequence of this influence is the so-called patterning effect: dependence of information transmission quality on the nature of the information [5–11]. The effect shows up most clearly in the error statistics table for various elementary bit sequences. Knowledge of the distribution of bit error statistics in data transmission through FOCLs is of importance in developing direct error correction schemes. The use of such information in error correction schemes, proposed by Shafarenko et al. [7], was successfully demonstrated in Refs [8–11]. Such schemes can improve signal detection quality when signal distortions cannot be compensated by active components of the system. Distortions may originate from a variety of physical effects. For example, in the case of on/off keying (OOK) (binary intensity modulation data transmission format) four-wave mixing produces 'ghost pulses' [12–16]. Such pulses are a spectacular example of the patterning effect in optical channels, where the single-bit error probability depends on the neighbouring bits. In particular, earlier results [6] demonstrate that, in the OOK format, bit combinations containing the 101 sequence have the highest probability to be received with an error in the central zero. From analysis of the error statistics for binary differential phase modulation in Ref. [8], it follows that, in this case, the central bits in the 010 and 101 sequences are the most error-prone.

Modern FOCLs ensure information transmission at tens of terabits per second through hundreds of WDM channels, each with a transmission capacity of up to 100 Gbit s^{-1} [17, 18]. One of the key questions to be answered in this context is how an increase in signal power – inevitable when the number of WDM channels in the link increases – influences the signal transmission quality in individual channels. In the case of binary modulation formats and low data rates, this issue has been addressed in great detail [8, 19] and information transmission quality has been shown to depend on the nature of the information: errors in various binary sequences have nonuniform statistics. No such studies have been carried out for nonbinary formats. Since these underlie modern FOCL design concepts, the study of such formats allows one to describe the key features of their application and find solutions capable of improving the information transmission quality at high transmission capacities.

This paper addresses the mathematical modelling of information (optical signal) transmission through an FOCL at a rate of 80 Gbit s^{-1} (40 GBd) per WDM channel using a four-level phase modulation format (QPSK). We present results of direct signal detection at the receiver end and derive the error distribution for various symbol combinations, which demonstrates a strong patterning effect.

A.A. Redyuk, A.S. Skidin Institute of Computational Technologies, Siberian Branch, Russian Academy of Sciences, prosp. Akad. Lavrent'eva 6, 630090 Novosibirsk, Russia; e-mail: redyuk@ict.sbras.ru, ask@skidin.org;
A.V. Shafarenko University of Hertfordshire, College Lane, Hatfield, Hertfordshire, AL10 9AB, UK; e-mail: a.shafarenko@herts.ac.uk;
M.P. Fedoruk Institute of Computational Technologies, Siberian Branch, Russian Academy of Sciences, prosp. Akad. Lavrent'eva 6, 630090 Novosibirsk, Russia; Novosibirsk State University, ul. Pirogova 2, 630090 Novosibirsk, Russia; e-mail: mife@ict.nsc.ru

Received 6 April 2012; revision received 14 May 2012
Kvantovaya Elektronika **42** (7) 645–649 (2012)
Translated by O.M. Tsarev

2. System configuration

Numerical simulation was performed for the transmission link schematically shown in Fig. 1. Each periodic section of the link comprises a 85-km length of standard single-mode fibre (SMF) and a span of dispersion-compensating fibre (DCF), which compensates the chromatic dispersion in the SMF. The DCF length, 14.45 km, is such that the average dispersion of the section is zero. This transmission link is a widespread controlled-dispersion system. The key parameters of the fibres are as follows:

	SMF	DCF
Loss at 1550 nm/dB km^{-1}	0.2	0.65
Dispersion/ps nm^{-1} km^{-1}	17	–100
Dispersion slope/ps nm^{-2} km^{-1}	0.07	–0.41
Nonlinearity coefficient/km W^{-1}	1.37	5.76

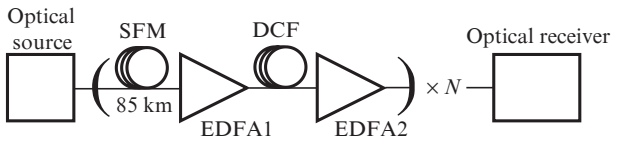

Figure 1. FOCL configuration.

Full compensation of the optical loss in each section was ensured by two erbium-doped fibre amplifiers (EDFAs). The gain coefficient G and noise figure (NF) of both were 13.2 and 4.5 dB, respectively. The number of sections in the link, N, was varied from 1 to 30. Next, a receiver was simulated.

Information was transmitted in the QPSK format, in which the phase of an optical carrier depends on the data being transmitted, while its amplitude and frequency are maintained constant. The vector diagram of this format is presented in Fig. 2. When four phases equidistant on a circle are used for encoding, every pulse can represent two information bits. Thus, one can either double the data rate per WDM channel relative to binary formats at a given passband or reduce the bandwidth by a factor of two, while maintaining the data rate unchanged.

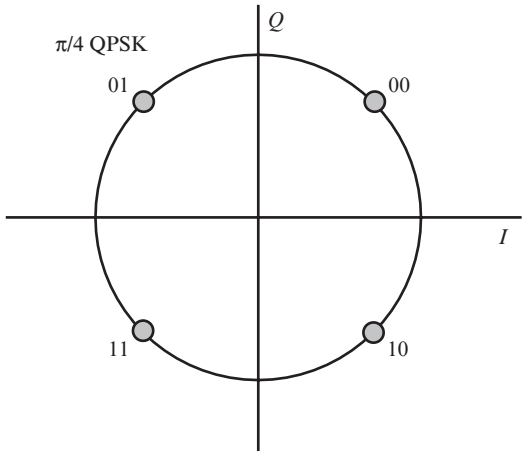

Figure 2. Vector diagram of the QPSK format.

3. Mathematical models

A key component of FOCLs is an optical transmitter. Every symbol coming to its input is converted to an optical pulse with particular characteristics. In the QPSK format, both the shape of the envelope (profile) and the frequency of the optical signal are the same for all the symbols, whereas the magnitude of its phase can take four values, depending on the symbol being transmitted, which consists of a pair of bits. Such pairs are mapped into symbols using Gray coding, according to which neighbouring symbols differ only by one bit (Fig. 2). In our calculations, we used pulse profiles of the form $A(t) = \frac{1}{2}\sqrt{P_0}\,[1 + \cos(2\pi t/T)]$, where P_0 is the initial peak pulse power; T is the symbol duration; and $t \in [-T/2; T/2]$. At a symbol rate of 40 GBd, we have $T = 25$ ps. The peak power in numerical simulations was taken to be 1 or 10 mW. These values were chosen experimentally and correspond to two signal propagation modes. In the former case, signal distortions are mainly due to the noise in the amplifiers. The latter case is of greater interest because future developments in FOCLs will build on an increase in the signal power coupled into the fibre and compensation of the nonlinear distortions at the receiver.

The propagation of an optical signal through a fibre can be described by the generalised nonlinear Schrödinger equation for the complex-valued envelope of the electromagnetic field $A(z,t)$ [20–22]:

$$\mathrm{i}\frac{\partial A}{\partial z} - \frac{\beta_2}{2}\frac{\partial^2 A}{\partial t^2} - \mathrm{i}\frac{\beta_3}{6}\frac{\partial^3 A}{\partial t^3} + \gamma |A|^2 A = -\mathrm{i}\frac{\alpha}{2}A. \qquad (1)$$

Here, z is a coordinate along the fibre; t is time; β_2 is the group velocity dispersion; β_3 is the third-order dispersion; α is the attenuation coefficient; $\gamma = k_0 n_2/A_{\mathrm{eff}}$ is the nonlinearity coefficient; n_2 is the nonlinear refractive index of the fibre; $\lambda_0 = 2\pi/k_0 = 1550$ nm is the carrier wavelength; and A_{eff} is the effective mode area of the fibre. Equation (1) can be solved numerically using splitting according to physical processes and the fast Fourier transform [22].

Erbium-doped fibre amplifiers were modeled by a point device which multiplied the amplitude of the optical signal by $\sqrt{G}$ and added a spontaneous emission noise. Noise was described using an additive white Gaussian noise model. The white noise spectral density can be evaluated as $S_{\mathrm{sp}} = (G-1)n_{\mathrm{sp}}h\nu_0$, where h is the Planck constant; ν_0 is the signal carrier frequency; and n_{sp} is the spontaneous emission coefficient, related to the noise factor of the amplifier by $\mathrm{NF} = 2n_{\mathrm{sp}} \times (G-1)/G$.

To filter off the spontaneous emission noise generated by the optical amplifiers, an optical filter was placed at the receiver end of the FOCL, which was used to multiply the amplitude – frequency distribution, $A(\omega)$, by its transfer function. The function was Gaussian in shape with a unity amplitude at a frequency $\omega_0 = 2\pi c/\lambda_0$. Calculations were performed for a filter with a bandwidth at half maximum of 110 GHz.

After optical filtering, the signal arrives at the receiver, which converts each pulse to a symbol. The direct detection procedure is as follows: For each pulse, its phase is calculated in the middle of time interval T as $\varphi = \arctan[\mathrm{Im}A(t)/\mathrm{Re}A(t)]$. The calculated phase is then used to decide according to Table 1 which symbol corresponds to the pulse. Next, the received symbol sequence is compared to the initial sequence and errors are analysed.

The spontaneous emission noise in the amplifiers and nonlinear effects distort the pulse shape and phase, resulting

Table 1. Correspondence between phases and symbols.

Phase	Symbol
$0 < \varphi < \pi/2$	00
$\pi/2 < \varphi < \pi$	01
$\pi < \varphi < 3\pi/2$	11
$3\pi/2 < \varphi < 2\pi$	10

in errors at the receiver end. Moreover, nonlinear effects lead to a phase shift, which accumulates as the signal propagates along the fibre. Figure 3 illustrates the phase shift for three periodic sections of a transmission link. The phase shift is proportional to the signal power and propagation distance and may, under certain conditions, be the main cause of errors at the receiver. Because of this, most FOCLs employ differential phase modulation formats, in which information is encoded using not the magnitude of the phase but the phase difference between two consecutive pulses. In the case of nondifferential phase modulation formats and coherent detection, one has to reconstruct the phase. This can be done at the receiver end using digital signal processing algorithms. It is also worth noting that the subject of this study is the received signal amplitude profile, which is independent of the signal phase.

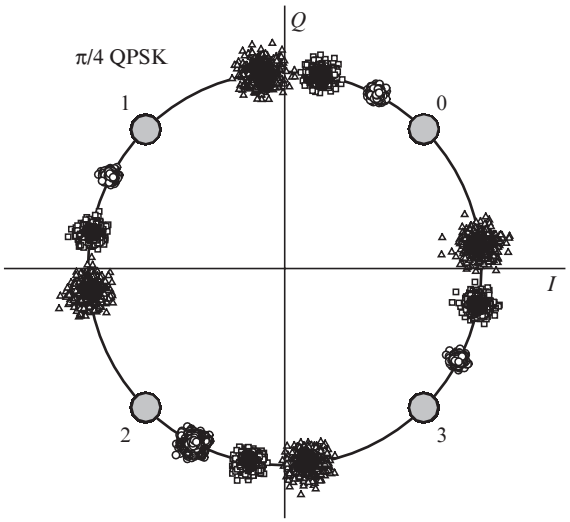

Figure 3. Vector diagram of the QPSK format. The large shaded circles show the initial phase, and the open data points show the phase after one (circles), two (squares) and three (triangles) sections.

4. Numerical simulation results

Here we consider the results of numerical simulations for the propagation of optical pulses through an FOCL with the use of the four-level phase modulation format. The key parameters used in the calculations were as follows:

Symbol rate/GBd 40
Bit rate/Gbit s^{-1} 80
Sequence length (symbols) . . . . . 2^{15}
Number of points per pulse 32
Carrier wavelength/nm 1550
Number of sections (N) 1–30
Section length/km 100

We performed a total of 50 numerical simulations with various initial symbol sequences and various random amplifier noise implementations. In each simulation, we used a pseudorandom sequence of 2^{15} symbols. After each periodic section, direct signal detection was performed as described above. Next, the results were averaged over all simulations.

Let us dwell on the simulation results for a propagation distance of 1400 km. This distance should be considered separately for two reasons: First, it is typical of medium- and long-haul communication systems. Second, the bit error rate obtained, 10^{-3}, approaches the threshold for direct error correction schemes. In the symbol sequences obtained after the detector, we identified bit errors and performed triplet analysis, i.e. analysis of groups of three consecutive symbols. An error in a triplet was determined by an error in the central bit. In the four-level format, use is made of four states of the phase in the vector (symbol) diagram and, hence, of four different symbols, so there are 64 ($4 \times 4 \times 4$) different triplets. Since each triplet corresponds to its own set of three pulses, it is reasonable to expect that the central pulse in each triplet will have special distortions as a result of propagation. It has been found, however, that all the triplets can be divided into several classes within which they are identical from the viewpoint of the phase profile of the corresponding pulses. For example, the 000, 111, 222 and 333 triplets have identical phase profiles, displaced by $\pi/2$ relative to one another. Numerical simulation results demonstrate that such triplets can have errors with equal probabilities. As a result, 16 different classes can be identified, instead of the original 64 triplets. Table 2 shows the number of errors in triplets for the 16 classes after 1400-km signal propagation. The total error count is 2168, which corresponds to a bit error rate of 10^{-3}.

Table 2. Triplet error distribution.

Triplet class	Error count	Percent of errors
000&111&222&333	364	16.79
020&131&202&313	352	16.24
001&112&223&330	96	4.43
021&132&203&310	121	5.58
002&113&220&331	13	0.6
022&133&200&311	16	0.74
003&110&221&332	98	4.52
023&130&201&312	57	2.63
010&121&232&303	17	0,78
030&101&212&323	17	0.78
011&122&233&300	92	4.24
031&102&213&320	64	2.95
012&123&230&301	350	16.14
032&103&210&321	294	13.56
013&120&231&302	124	5.72
033&100&211&322	93	4.29

It can be seen from Table 2 that the errors are unevenly distributed over the classes. Some of the triplets (e.g. 000) make a large contribution to the total error count, whereas the contribution of others (e.g. 002) is, by contrast, negligible. When numerical simulations were carried out for 1-mW peak power pulses, the error distribution was essentially uniform. The reason for this is that, in the case of pulses with a low initial power, the main error source is the amplifier noise, which distorts all pulses to the same extent. In the case of higher power pulses, nonlinear effects become more important, which have different effects on different pulse sequences, well illustrating the patterning effect.

To account for the uneven error distribution, we examined three different triplets: 000 (one of the largest error counts), 002 (one of the smallest error counts) and 001 (small error count). To this end, we simulated the propagation of a pseudorandom sequence of 2^{15} symbols over a distance of 1400 km along a FOCL whose configuration was described above. To assess the influence of nonlinear effects, the simulation included noise-free amplifiers. Figure 4 shows eye diagrams of the pulse power profile for three triplets. It is seen that, in the case of the 000 triplet, the power of the inner pulse decreases, whereas that of the outer pulses rises (for convenience, we indicate the total pulse energy averaged over all the 000 triplets in the sequence). In contrast, the power of the inner pulse in the 002 triplet increases and that of the outer pulses drops.

Figure 5 shows the vector diagrams for the same triplets. Each data point in the diagrams represents the phase and amplitude of the inner pulse calculated in the middle of the symbol interval. From the signal phase, the detector decides which symbol corresponds to the received signal. A triplet will be erroneous if the corresponding point in the diagram will lie beyond the first quadrant. As seen in the diagram, the cloud of the 000 triplet is extended along the circle, whereas that of the 002 array is extended in radial direction. This accounts for the fact that errors are encountered much more frequently in the 000 triplet than in the 002 triplet: when extended along the circle, a phase cloud leaves the correct detection region before clouds extended in radial direction. It is worth pointing out that most of the data points of the 000 triplet lie within the circle. This is indirect evidence that the average energy of the inner pulse in this triplet is lower than that of the outer pulses. The phase cloud of the 001 triplet, which is responsible for a medium number of errors (Table 2), is intermediate in state between the clouds of the triplets extended along the circle and in radial direction.

The present mathematical modelling results demonstrate that, as the pulse peak power increases from 1 to 10 mW, the signal transmission quality begins to depend on the type of signal (Table 2). Since uneven error statistics were observed as well earlier for binary modulation formats (for intensity [19] and phase [8] modulation), we are led to conclude that this effect persists for formats with higher spectral efficiency in comparison with the binary formats. Such statistics can be taken into account in information encoding methods proposed in recent years and intended for optical communication channels [10, 11, 15]. Such information can also be applied in designing detectors that will take into account not only the phase of the signal in the phase plane but also secondary parameters, e.g. the amplitude of a given pulse relative to its neighbours (Fig. 4).

5. Conclusions

We carried out mathematical modelling of information transmission through an FOCL at a rate of 80 Gbit s^{-1} (40 GBd) per WDM channel using optical pulses and a four-level phase modulation format. Based on direct optical signal detection, we analysed error statistics and identified an uneven error dis-

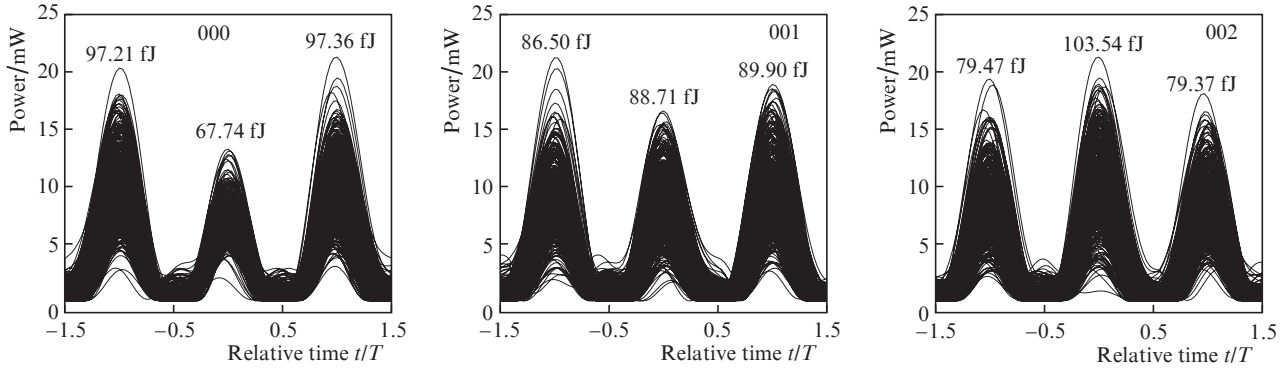

Figure 4. Eye diagrams of the pulse power profile for the 000, 001 and 002 triplets.

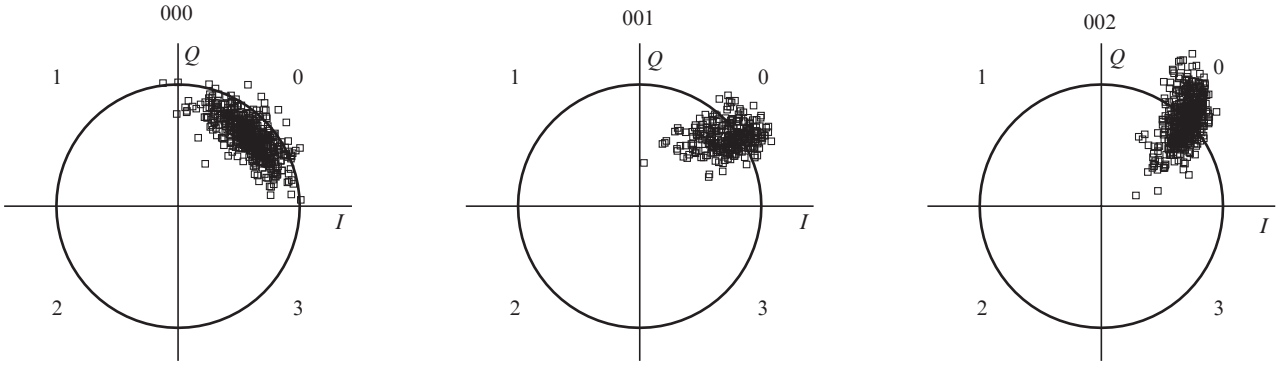

Figure 5. Vector diagrams for the 000, 001 and 002 triplets.

tribution over triplets. We examined the influence of nonlinear effects on the optical pulse profile and that of neighbouring pulses on the distortion of a given pulse.

Acknowledgements. This work was supported by the RF Ministry of Education and Science (State Contract Nos 11.519.11.4018 and 11.519.11.4001).

References

1. Nagayama K., Saitoh T., Kakui M. *Proc. OFC* (Anaheim, 2002).
2. Winzer P.J., Essiambre R.-J. *Proc. IEEE*, **94**, 952 (2006).
3. Okoshi T., Kikuchi K. *Coherent Optical Fiber Communications* (Tokyo: KTK, 1988).
4. Derr F. *Electron. Lett*., **27** (23), 2177 (1991).
5. Settembre M., Matera F., Hagele V., et al. *J. Lightwave Technol*., **15** (6), 962 (1997).
6. Shapiro E.G., Fedoruk M.P., Turitsyn S.K. *Electron. Lett*., **37** (19), 1179 (2001).
7. Shafarenko A., Turitsyn K.S., Turitsyn S.K. *IEEE Trans. Commun*., **55** (2), 237 (2007).
8. Turitsyn S.K., Fedoruk M.P., Shtyrina O.V., et al. *Opt.Commun*., **277** (2), 264 (2007).
9. Slater B., Boscolo S., Shafarenko A., Turitsyn S.K. *J. Opt. Networking*, **6** (8), 984 (2007).
10. Skidin A., Redyuk A., Shtyrina O., et al. *Opt. Commun*., **284** (19), 4695 (2011).
11. Shafarenko A., Skidin A., Turitsyn S.K. *IEEE Trans. Commun*., **58** (10), 2845 (2010).
12. Essiambre R.-J., Mikkelsen B., Raybon G. *Electron.Lett*., **35** (18), 1576 (1999).
13. Mamyshev P.V., Mamysheva N.A. *Opt. Lett*., **24** (21), 1445 (1999).
14. Shake I., Takara H., Mori K., et al. *Electron. Lett*., **34** (16), 1600 (1998).
15. Rao V.S., Djordjevic I.B., Vasic B. *IEE Proc. Optoelectron*., **153** (2), 87 (2005).
16. Shapiro E.G., Fedoruk M.P., Turitsyn S.K., Shafarenko A. *IEEE PTL*, **15** (10), 1473 (2003).
17. Qian D. et al. *Proc. OFC/NFOEC* (Los Angeles, 2011).
18. Yu J. et al. *Proc. OFC/NFOEC* (Los Angeles, 2011).
19. Shapiro E.G., Fedoruk M.P., Turitsyn S.K. *Electron.Lett*., **40** (22), 1436 (2004).
20. Hasegawa A., Tappert F. *Appl. Phys. Lett*., **23**, 142 (1973).
21. Zakharov V.E., Shabat A.T. *Zh. Eksp. Teor. Fiz*., **61** (1), 118 (1971).
22. Agrawal G.P. *Nonlinear Fiber Optics* (San Diego: Academic, 1995; Moscow: Mir, 1996).